MI108: Ultrasonic Imaging, Tomography, and Therapy

Whole breast tissue characterization with ultrasound tomography

Neb Duric[1,2], Peter Littrup[1,2], Cuiping Li[1,2], Olivier Roy[1,2], Steven Schmidt[1,2], John Seamans[2], Andrea Wallen[2] and Lisa Bey-Knight[1].

[1]Karmanos Cancer Institute, Wayne State University, Detroit, MI

[2]Delphinus Medical Technologies, Plymouth MI

Abstract: A number of clinical trials have shown that screening ultrasound, supplemental to mammography, detects additional cancers in women with dense breasts. However, labor intensity, operator dependence and high recall rates have limited adoption. This paper describes the use of ultrasound tomography for whole-breast tissue stiffness measurements as a first step toward addressing the issue of high recall rates. The validation of the technique using an anthropomorphic phantom is described. In-vivo applications are demonstrated on 13 breast masses, indicating that lesion stiffness correlates with lesion type as expected. Comparison of lesion stiffness measurements with standard elastography was available for 11 masses and showed a strong correlation between the 2 measures. It is concluded that ultrasound tomography can map out the 3 dimensional distribution of tissue stiffness over the whole breast. Such a capability is well suited for screening where additional characterization may improve the specificity of screening ultrasound, thereby lowering barriers to acceptance.

INTRODUCTION

Mammography is the currently accepted gold standard for breast screening. Mammography detects about 2 to 4 cancers per 1000 screens [1] but has a relatively low positive predictive value (PPV). Sensitivity of mammography may be only about 50% in women with dense breast tissue [2], women who are at particularly high risk for developing breast cancer [3-7]. Screening studies utilizing whole breast ultrasound have shown a significant increase in the detection of cancers of up to 4 additional cancers per 1000 screens thereby validating ultrasound's known superior performance in dense tissue [8]. A striking aspect of the added detections is that they are predominantly node negative invasive cancers that could have progressed to a later stage before possible mammographic detection. However, ultrasound's increased sensitivity to invasive cancer is potentially offset by lowered sensitivity to *ductal carcinoma in situ* (DCIS) by virtue of mammography's greater ability to detect microcalcifications. Although such a trade-off may be justified by the fact that mortality from invasive cancers is much higher than that from DCIS, a combined screening (mammography plus whole breast ultrasound) would provide a comprehensive screen. It has therefore been proposed that whole breast ultrasound be used for screening, supplemental to mammography. The SomoInsight screening study indeed showed that whole breast ultrasound plus mammography outperformed mammography alone [9], leading to the first FDA approval for ultrasound screening for breast cancer. Unfortunately, adoption of ultrasound screening has been slow. One possible reason is that ultrasound screening increases call back rates (up to a factor of 2 in case of the SomoInsight study). Improved lesion characterization would therefore help lower the barriers to adoption of screening ultrasound.

Figure 1. The SoftVue System.

Ultrasound tomography (UST) is an emerging technique that moves beyond B-mode imaging by virtue of its through transmission capabilities [10-23]. Transmission ultrasound provides additional

characterization by measuring tissues parameters such as sound speed and attenuation.

These parameters can be used to characterize tissue stiffness across an entire coronal section of the breast and summed into a 3D volume, capabilities not available in current whole breast ultrasound systems. A combination of sound speed and attenuation to render relative "stiffness" across an entire breast slice thereby addresses potential improved detection of subtle suspicious masses (i.e., sensitivity) while de-emphasizing the larger number of masses suggested by standard reflection US alone (i.e., specificity). The method is illustrated in Figure 2.

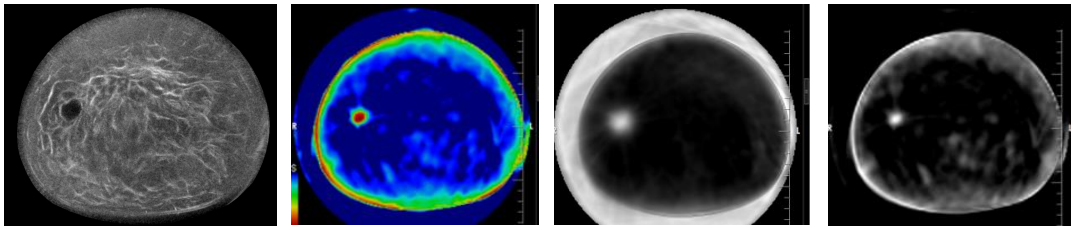

Figure 2. Imaging modes of the SoftVue System. Far left shows the B-mode imaging. The colored stiffness map is made by combining the sound speed and attenuation images.

The purpose of this paper is to present the results of a study aimed at demonstrating UST's ability to characterize tissue stiffness throughout the breast, as a first step toward additional lesion characterization for possible reduction in call back rates.

METHODS

The SoftVue system utilizes a ring shaped transducer that collects not only backscattered signals but also through-transmission signals [24]. SoftVue uses the backscattered signals to produce B-mode (grey-scale) images of the breast. The through-transmission signals are used to calculate maps of the speed of sound and attenuation. Since these parameters carry information about tissue density and stiffness [25], it is hypothesized that combining them can yield maps of tissue stiffness. SoftVue represents these stiffness maps in the form of color images. This hypothesis was tested by generating such images from both phantom and clinical in-vivo data to determine whether this measure of tissue stiffness correlates with known properties of breast masses. The stiffness measurements were then compared with elastography measurements made with a Toshiba Aplio 500 hand-held ultrasound probe to determine whether this technique for measuring tissue stiffness correlates with current basic elastography measurements. Color representation of SoftVue images was similar to that of the Toshiba, using red for stiff and blue for soft tissues.

Initial baseline measurements were made of an anthropomorphic breast phantom for technique validation. The phantom contained inclusions mimicking cancers, fibroadenomas and cysts. Table 1 lists the inclusions used. The phantom was scanned with a clinical UST prototype, SoftVue, built by Delphinus Medical Technologies, Plymouth MI, shown in Fig 1. The resulting B-mode and stiffness images were stored for comparison with known properties of the phantom inclusions.

Table 1: Anthropomorphic Breast Phantom: Known mass properties

Phantom component	Number/Size	Sound Speed (m/s)	Attenuation coefficient at 2.5 MHz (dB/cm)	Stiffness
Cyst	2/ 8mm - 12mm	1548	0.07	Soft
Fibroadenoma	2/ 8mm - 12mm	1552	0.52	Stiff
Cancer	2/ 8mm – 12mm	1563	1.20	Stiff

After initial validation, the technique was tested with clinical, in-vivo data. Study subjects were recruited under a HIPAA compliant, IRB approved study at the Karmanos Cancer Institute (KCI), Detroit MI. Symptomatic patients were scanned with SoftVue. Patient data were selected to include the most common benign breast masses, as well as

cancers (Table 2). The resulting B-mode and stiffness images were stored for comparison with their known properties from pathological correlation, based on biopsy results and standard imaging.

A total of 13 in-vivo masses were imaged, representing a variety of breast lesions in patients whose breast density ranges from fatty to dense [Breast Imaging-Reporting and Data System (BI-RADS) breast composition categories 1 to 4, respectively].

Table 2: In Vivo Masses Used for Image Characterization

Mass Type	Number/Size	Possible measurements
Cyst	5 (10mm – 25mm)	1. Soft (bluer than background on average) 2. Mixed (can be stiff or soft) 3. Stiff (redder than background on average)
Fibroadenoma	4 (10mm- 45mm)	
Cancer	4 (10mm – 30mm)	

SoftVue's B-mode imaging was chosen to make the initial mass identification and provide a reference for relevant regions of interest. ImageJ software was used to display all SoftVue images to assist with the image comparisons. ImageJ was developed by NIH and is a public domain, full-featured standalone diagnostic viewer. The Philips iSite Software Package was used to display standard patient imaging (e.g. mammography and hand held ultrasound), when necessary, to help the radiologist determine lesion position and location. A semi-transparent overlay of the SoftVue color images was displayed to ease the identification of regions of interest when doing the comparison. A clinical interpretation of each image was provided by a board certified radiologist. Pathology and/or radiology reports were used as the ground truth for verifying lesion type and lesion location. The acceptance criteria for the phantom and in-vivo analysis were that the estimated colors and stiffness estimates of all the masses agree qualitatively with their known properties.

RESULTS

The phantom scan yielded SoftVue images of 7 inclusions. Among the 7 phantom inclusions, 1 cancer and 3 fibroadenomas were found to be stiff (appearing red) compared to the background material while the 3 cysts were found to be soft (appearing blue) in complete concordance with the known properties of the phantom. These data are summarized in Table . An example of a typical phantom image is shown in Fig. 3.

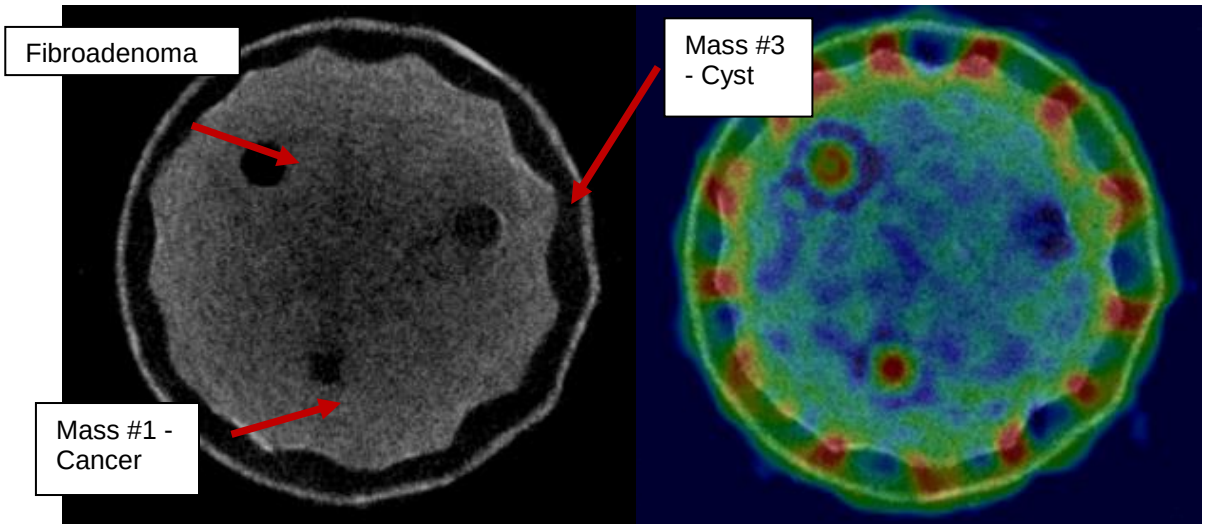

Figure 3: [Left] The B-mode image. **[Right]**. SoftVue color image overlaid (fused) on the grey scale B-mode image The overlay image shows that the fibroadenoma and cancer have more red (stiffer) while the cyst is blue (soft)

Table 3: Phantom Study Summary					
Mass ID #	**Size (mm)**	**Mass Type**	**Clock Position**	**Stiffness Estimate**	**True Stiffness (from Manufacturer)**
1	12mm	Cancer	7:00	Stiff	Stiff
2	12mm	Fibroadenoma	10:00	Stiff	Stiff
3	12mm	Cyst	2:00	Soft	Soft
4	8mm	Fibroadenoma	12:00	Stiff	Stiff
5	8mm	Cyst	4:00	Soft	Soft
6	8mm	Fibroadenoma	10:00	Stiff	Stiff
7	8mm	Cyst	2:00	Soft	Soft

The in-vivo data are summarized in Table 4. All 4 cancers were characterized as "stiff" by SoftVue's color images. Two fibroadenomas were found to be mixed (range of colors), 1 was stiff (red) and 1 was found to be soft (blue). Of the 5 cysts, 4 were found to be soft while 1 was found to be mixed.

Table 4: In-Vivo Study Summary						
Study #	**Breast Size**	**Breast Density**	**Lesion Pathology**	**Reported Lesion Position**	**Average Lesion Size (cm)**	**SoftVue stiffness assessment**
SV021	C	Dense	Cancer	8:00	2.5	Stiff
SV022	DD	Scattered	Fibroadenoma	1:30	3.0	Stiff
SV045	C	Scattered	Cancer	10:00	1.8	Stiff
SV077_1	B	Extremely Dense	Cyst	2:00	1.4	Soft
SV077_2	B	Extremely Dense	Cyst	12:00	1.9	Soft
SV077_3	B	Extremely Dense	Cyst	12:00	2.0	Soft
SV079	C	Heterogeneous	Cyst	9:00	1.4	Soft
SV089	D	Scattered	Cancer	9:30	1.7	Stiff
SV090	DDD	Heterogeneous	Fibroadenoma	10:00	4.3	Mixed
SV113	DD	Scattered	Cyst	2:00	1.8	Mixed
SV114	D	Scattered	Cancer	10:00 RA	1.2	Stiff
SV117_1	D	Dense	Fibroadenoma	5:00	1.9	Mixed
SV117_2	D	Dense	Fibroadenoma	8:00	2.6	Soft

Fig 4 shows representative in-vivo images of an irregular cancer with associated architectural distortion (Top), a stiff but well circumscribed fibroadenoma (Middle) and a cyst (Bottom). In each case, the B-mode image is shown on the left while the color stiffness image is shown on the right

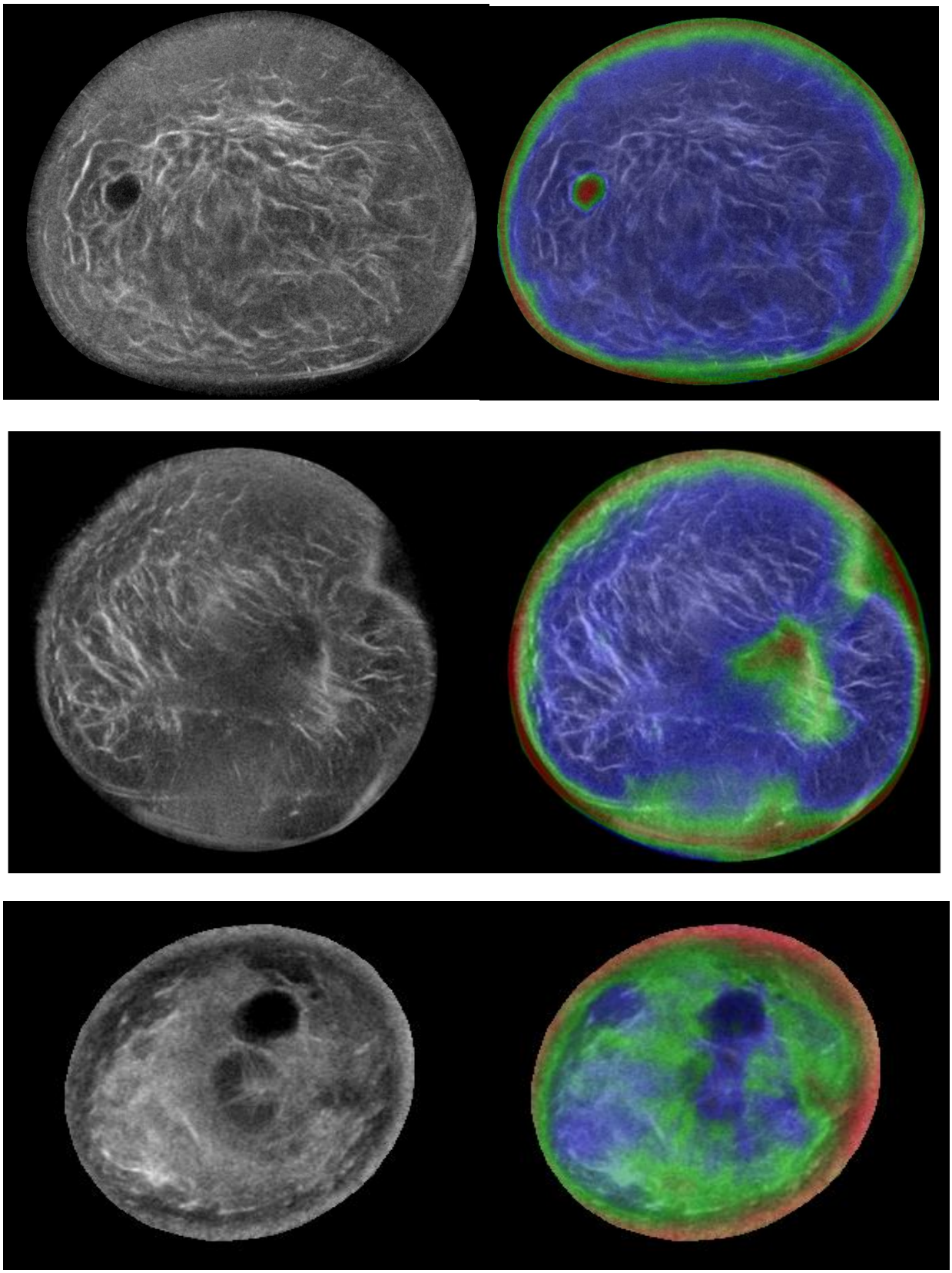

Figure 4. (Top) Full coronal B-mode image shows a cancer at 2:00 o'clock (left) with corresponding stiffness overlay (right). (Middle). A fibroadenoma at 9:00 o'clock and (Bottom) A cyst at 1:00 o'clock.

Elastography measurements were available for 11 masses. SoftVue stiffness measurements were compared with the elastography measurements and the results summarized in Table 5.

Table 5: Comparison with Elastography

Comparison #	Breast Size	Breast Density	Lesion Pathology	SoftVue Stiffness Estimate	Toshiba Stiffness Estimate	Lesion Size (cm)
1	DD	Scattered	Cancer	Stiff	Stiff	2.6
2	B	Scattered	Fibroadenoma	Stiff	Stiff	2.9
3	DD	Scattered	Fibroadenoma	Mixed	Mixed	1.6
4	B	Extremely Dense	Cyst	Soft	Soft	1.4
5	B	Extremely Dense	Cyst	Soft	Soft	1.9
7	DDD	Heterogeneous	Fibroadenoma	Stiff	Stiff/Mixed	4.3
8	B	Scattered	Cancer	Stiff	Stiff	1.4
9	A/B	Heterogenous	Cancer	Stiff	Stiff	2.3
10	D	Scattered	Cancer	Stiff	Stiff	1.2
11	D	Dense	Fibroadenoma	Mixed	Mixed	1.9

DISCUSSION

Fig 5 shows the distribution of stiffness properties by lesion type according to the SoftVue measurements. The lesion stiffness characteristics show trends that indicate cancers to be on average stiff compared to surrounding tissue, while cysts appear "soft". Fibroadenomas can be either stiff or soft or can have characteristics of both. These trends are consistent with known properties of breast masses.

In traditional US imaging, mass stiffness is characterized by its elastic properties, as measured by elastography. To determine whether SoftVue's method of measuring stiffness is consistent with elastography measurements, we compared the two types of measurements in 11 cases where both measurements were available. As shown in Table 5, there was strong qualitative agreement between the two sets of measurements suggesting that the two different systems measure similar lesion properties despite using very different techniques.

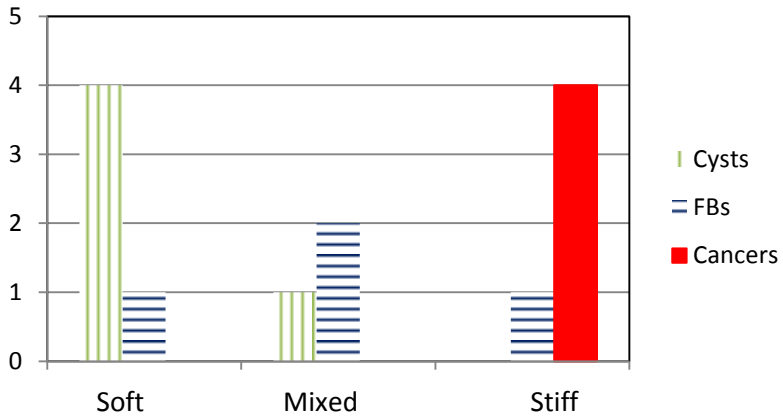

Figure 5. Histogram of stiffness values by tumor type.

The SoftVue system uses through transmission to characterize stiffness by virtue of how longitudinal sound waves propagate through tissue. The Toshiba Aplio 500 uses elastography to assess whether a lesion is hard or soft. Despite the two widely different methods, the two sets of measurements correlate well qualitatively. One possible

explanation is that the global elastic properties of lesions drive the propagation of longitudinal waves in a similar manner and may be mediated by a correlation between density and stiffness which at least for breast tissue appears to hold (Maast, 2000). Thus, a hard lesion, for example, is also a dense lesion which supports high sound speed. On the other hand, a non-solid lesion is characterized by low levels of attenuation to longitudinal waves. Therefore, combining attenuation and sound speed into a single stiffness parameter yields low values of stiffness for non-solid lesions such as cysts and high stiffness values for solid lesions such as cancers.

CONCLUSIONS

It is shown that breast imaging with a ring transducer array, as embodied by the SoftVue system, can be used to provide maps of tissue stiffness throughout the volume of the breast by combining maps of sound speed and attenuation. The method was validated on an anthropomorphic phantom, clearly showing distinct stiffness properties relative to surrounding tissue. This capability was applied in-vivo to a variety of breast masses and shown to yield relative stiffness assessments that correlate well with known tumor properties. In-vivo validation was demonstrated by correlating stiffness measurements with elastography measurements using a hand held probe. It is concluded that tissue characterization using through transmission ultrasound can be used to assess lesion stiffness. Furthermore, the ability to map stiffness of the whole breast enables the concept to be applied in a screening scenario.

Strengths and Limitations of this study. The study described in this paper is a proof of concept study and is defined by a small sample size. Hence, the correlations described above are not sufficiently powered to justify broad conclusions about the accuracy of the technique. Similarly, the stiffness measurements presented in this paper are qualitative and based on a visual assessment of the appearance of a lesion relative to its surroundings. Nevertheless, the study does demonstrate that tissue characterization of lesions using through transmission tomography is feasible. Furthermore, it is shown that this approach delivers tissue characterization throughout the volume of the breast, something that is currently not possible with other ultrasound devices.

ACKNOWLEDGMENTS AND DISCLOSURES

The authors acknowledge the support of the National Cancer Institute through grant 1R44CA165320-01A1. N. Duric and P. Littrup are co-founders of Delphinus Medical Technologies Inc. and are performing the clinical studies relating to SoftVue under a financial conflict of interest plan that has been approved by Wayne State University.

REFERENCES

[1] SEER website. http://seer.cancer.gov/

[2] American Cancer Society. *Cancer Prevention & Early Detection Facts & Figures 2009*. Atlanta, GA: American Cancer Society, 2009; 34-37. Boyd NF, Guo H, Martin LJ, Sun L, Stone J, Fishell E, Jong RA, Hislop G, Chiarelli

[3] Chen J, Pee D, Ayyagari R, Graubard B, Schairer C, Byrne C, Benichou J, Gail MH: Projecting absolute invasive breast cancer risk in white women with a model that includes mammographic density. *J Natl Cancer Inst* 2006, 98:1215-1226.

[4] Ursin G, Hovanessian-Larsen L, Parisky YR, Pike MC, Wu AH: Greatly increased occurrence of breast cancers in areas of mammographically dense tissue. *Breast Cancer Res* 2005, 7:R605-R608.

[5] Martin LJ, Boyd N: Potential mechanisms of breast cancer risk associated with mammographic density: hypotheses based on epidemiological evidence. *Breast Cancer Res* 2008, 10:1-14.

[6] Armstrong K, Moye E, Williams S, Berlin JA, Reynolds EE. Screening mammography in women 40 to 49 years of age: a systematic review for the American College of Physicians. Ann Intern Med. 2007; 146:516-26

[7] A, Minkin S. et al.: Mammographic density and the risk and detection of breast cancer. *N Engl J Med* 2007, 356:227-236.

[8] Berg WA, Blume JD, Cormack JB, Mendelson EB, Lehrer D, Böhm-Vélez M, Pisano ED, Jong RA, Evans WP, Morton MJ, Mahoney MC, Hovanessian Larsen L, Barr RG, Farria DM, Marques HS, Boparai K, for the ACRIN 6666 Investigators. Combined Screening With Ultrasound and Mammography vs Mammography Alone in Women at Elevated Risk of Breast Cancer. JAMA 2008;299(18):2151-2163.

[9] Brem, R. F., Tabár, L., Duffy, S. W., Inciardi, M. F., Guingrich, J. A., Hashimoto, B. E., ... & Miller, D. P. (2014). Assessing improvement in detection of breast cancer with three-dimensional automated breast US in women with dense breast tissue: The SomoInsight Study. Radiology.

[10] Carson PL, Meyer CR, Scherzinger AL, Oughton TV. Breast imaging in coronal planes with simultaneous pulse echo and transmission ultrasound. Science 1981, Dec 4;214(4525):1141-3.

[11] Andre MP, Janee HS, Martin PJ, Otto GP, Spivey BA, Palmer DA, "High-speed data acquisition in a diffraction tomography system employing large-scale toroidal arrays," International Journal of Imaging Systems and Technology 1997;Vol. 8, Issue 1:137-147.

[12] Johnson SA, Borup DT, Wiskin JW, Natterer F, Wuebbling F, Zhang Y, Olsen C. *Apparatus and Method for Imaging with Wavefields using Inverse Scattering Techniques*. United States Patent 6,005,916 (1999).

[13] Marmarelis VZ, Kim T, Shehada RE. Proceedings of the SPIE: Medical Imaging; Ultrasonic Imaging and Signal Processing 2003, Paper 5035-6.

[14] Liu D-L, Waag RC. "Propagation and backpropagation for ultrasonic wavefront design," *IEEE Trans. on Ultras. Ferro. and Freq. Contr*. 1997;44(1):1-13.

[15] Gemmeke, H and Ruiter, N. "3D ultrasound computer tomography for medical imaging". *Nuclear instruments and methods in Physics Research Section A: Accelerators, Spectrometers, Detectors and Associated Equipment*, vol. 580, no. 2, pp 1057-1065, 2007.

[16] Nicole V. Ruiter, Georg Göbel, Lutz Berger, Michael Zapf and Hartmut Gemmeke, "Realization of an optimized 3D USCT", Proc. SPIE 7968, 796805 (2011)

[17] Duric N, Littrup P, Poulo L, Babkin A, Pevzner R, Holsapple E, Rama O, Glide C. Detection of Breast Cancer With Ultrasound Tomography: First Results with the Computerized Ultrasound Risk Evaluation (C.U.R.E) Prototype. Medical Physics Feb 2007; Vol 34 (2), pp. 773-785.

[18] Duric, N., Boyd, N., Littrup, P., Sak, M., Myc, L., Li, C., ... & Albrecht, T. (2013). Breast density measurements with ultrasound tomography: A comparison with film and digital mammography. Medical physics, 40, 013501

[19] Glide-Hurst C, Duric N, Littrup P. Volumetric breast density evaluation from ultrasound tomography images. Med Phys. 2008;Vol. 35, Issue 9, pp. 3988-3997.

[20] S. Schmidt, Z. Huang, N. Duric, C. Li and O. Roy. "Modification of Kirchhoff migration with variable sound speed and attenuation for acoustic imaging of media and application to tomographic imaging of the breast:. Med. Phys. 38, 998 (2011).

[21] C. Li, N. Duric, P. Littrup, L. Huang. In vivo Breast Sound-Speed Imaging with Ultrasound Tomography. Ultrasound in Medicine & Biology, Volume 35, Issue 10, Pages 1615-1628. 2009.

[22] Ranger B, Littrup P, Duric N, Chandiwala-Mody P, Li C, Schmidt S and Lupinacci J. Breast ultrasound tomography versus magnetic resonance imaging for clinical display of anatomy and tumor rendering: Preliminary results. AJR Am J Roentgenol Jan 2012; 198(1):233-9.

[23] Duric, N. et al. Ultrasound Tomography Systems for Medical Imaging, in Emerging Imaging in Medical Diagnosis and Therapy. 2012. Taylor &Francis, Editors: Mark A. Anastasio; Patrick La Riviere. CRC Press. [Review Article].

[24] Duric, Neb, Peter Littrup, Cuiping Li, Olivier Roy, Steven Schmidt, Xiaoyang Cheng, John Seamans, Andrea Wallen, and Lisa Bey-Knight. "Breast imaging with SoftVue: initial clinical evaluation." In SPIE Medical Imaging, pp. 90400V-90400V. International Society for Optics and Photonics, 2014.

[25] Mast, T. Douglas. "Empirical relationships between acoustic parameters in human soft tissues." Acoustics Research Letters Online 1, no. 2 (2000): 37-42.